

# Water Saturation Shift Referencing (WASSR) for chemical exchange saturation transfer experiments

M. Kim<sup>1,2</sup>, J. Gillen<sup>1,2</sup>, J. Zhou<sup>1,2</sup>, and P. C. van Zijl<sup>1,2</sup>

<sup>1</sup>Russell H. Morgan Department of Radiology and Radiological Sciences, Johns Hopkins University School of Medicine, Baltimore, MD, United States, <sup>2</sup>F.M. Kirby Center for Functional Brain Imaging, Kennedy Krieger Institute, Baltimore, MD, United States

**INTRODUCTION:** Chemical exchange saturation transfer (CEST) has recently emerged as an alternative contrast mechanism for MRI (1-5). In this approach, selective radiofrequency (RF) irradiation of exchangeable solute protons is detected through progressive saturation of the water signal consequential to chemical exchange, leading to tremendous enhancement in MRI sensitivity. CEST data are acquired by detecting water saturation as a function of frequency, called a Z-spectrum. To remove competing effects due to direct water saturation (DS) and conventional MT, an asymmetry analysis of the Z-spectrum with respect to the water frequency is generally needed. Such analysis, however, may lead to erroneous results when the water frequency differs between image voxels due to field inhomogeneity. Correct assignment of the center frequency is especially problematic when the irradiation frequency of the CEST solute is sufficiently close to the water frequency for the CEST effect to overlap with DS effect, such as may be the case at lower fields due to poor spectral resolution. We show that proper water referencing can be accomplished by acquiring DS images under the condition of negligible interference of conventional MT and CEST effects, a method we dubbed water saturation shift referencing (WASSR). We applied WASSR to the study of glycogen in phantom and muscle, where the hydroxyl (OH) protons have such a small chemical shift difference (0.75-1.2 ppm) with bulk water protons that the CEST peak can not be separated from DS at 3T. **MATERIALS AND METHODS: Phantom:** A 200 mM solution of bovine liver glycogen (Sigma, St. Louis, MO) was prepared by dissolving 4.98 g of glycogen in 151 ml of PBS (pH 7.3). **In vivo study:** Healthy subjects in the resting state were scanned after written informed consent. **MRI Acquisition:** All images were acquired using a 3T Achieva scanner (Philips Medical System, Best, The Netherlands) with body coil transmission, phased-array coil reception and high order shimming. For series of consecutive WASSR and glycoCEST scans, saturation was accomplished using a block pulse before the turbo spin echo (TSE) acquisition (see Fig. 1). For WASSR, a brief low power block pulse was calibrated to have sufficient DS effect, while minimizing any MT effects. For CEST/MT, a relatively long high power block pulse was chosen for maximum glycogen CEST (glycoCEST) effect (6). No prescan was done between the WASSR and CEST scans to maintain the same field reference conditions. Multi-slice **glycogen phantom** images were acquired using 23 offsets (WASSR, range: 0.44 to -0.44 ppm) and 45 offsets (CEST, range: 4 to -4 ppm). Imaging parameters: TSE factor = 34, TR/TE = 5000/ 11 ms, matrix = 128 x 122, FOV = 160 x 160 mm<sup>2</sup>, slice thickness = 5 mm, 3 slices, 5 mm gap. RF saturation pulses: 50 ms and 0.1  $\mu$ T for WASSR, and 500 ms and 1.5  $\mu$ T for CEST. Total scan times were 4 min. 15 sec. (WASSR) and 7 min. 55 sec. (CEST). Single-slice **human calf muscle** imaging was performed using 33 offsets for both WASSR (range: 1 to -1 ppm) and CEST (range: 4 to -4 ppm). Imaging parameters were the same as for the phantom study except for TR (3000 ms) and for RF saturation pulses (100 ms and 0.25  $\mu$ T for WASSR, and 500 ms and 0.75  $\mu$ T for CEST). Total scan time was 3 min. 33 sec. for each scan. **Data analysis:** A custom-written program in Matlab (Mathworks, Natick, MA, USA) was used. WASSR Z-spectra were fitted on a voxel-by-voxel basis using a 31<sup>st</sup>-order polynomial and re-synthesized with 0.5 Hz resolution. The minimum of the fitted curve in each voxel was assumed to be the water frequency and the frequency-difference with respect to 0 ppm (arbitrary water offset) was taken to be the frequency shift, creating a WASSR map. The CEST Z-spectra were also fitted on a voxel-by-voxel basis using a 15<sup>th</sup>-order polynomial and re-synthesized with 0.5 Hz resolution. For each voxel, CEST curves were shifted using the frequency shift from the WASSR map. The magnitude of the CEST effect was quantified as  $MTR_{asym} = S(-freq)/S_0 - S(freq)/S_0$  where  $S$  and  $S_0$  are the saturated and non-saturated intensities.

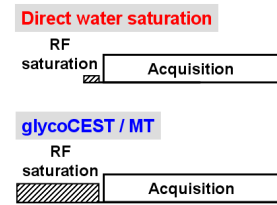


Fig. 1: WASSR and GlycoCEST schemes

**RESULTS AND DISCUSSION: Phantom Studies:** Fig. 2 shows  $MTR_{asym}$  images at 1 ppm offset from water. In panel A, a large spatial intensity fluctuation is visible while the corrected image (B) shows remarkable improvement in spatial homogeneity. The frequency variation over the whole phantom before correction was ~0.25 ppm. **Human Studies:** In Fig. 3A, a large spatial signal fluctuation is found. The DS Z-spectrum (Fig. 3C, blue line) from a selected ROI shows that the center frequency is shifted about ~0.039 ppm from water resulting in erroneous  $MTR_{asym}$  spike (Fig. 3C, red line). After applying the WASSR map in each voxel, the resulting glycoCEST images (Fig. 3D) look more homogeneous and show positive signal intensity within the expected frequency range for glycogen OH protons (0.75-1.25 ppm offset from water). The corresponding CEST spectrum (Fig. 3E, red line) indicates a glycoCEST effect of ~6%. Note that erroneous  $MTR_{asym}$  spike in the DS spectrum is gone (Fig. 3F, red line) after the proper centering. Overall, the WASSR map provides the absolute center frequency on a voxel-by-voxel basis while a typical field map (7) contains only relative frequency shifts, and can thus not perform this correction. In addition, the WASSR scan acquisition parameters are identical to CEST, avoiding a mismatch in image distortions between two data sets. **CONCLUSIONS:** We have demonstrated that the field variation leading to artifactual signal spikes in CEST images can be corrected using WASSR in which DS images are used as a center

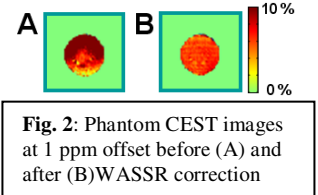


Fig. 2: Phantom CEST images at 1 ppm offset before (A) and after (B) WASSR correction

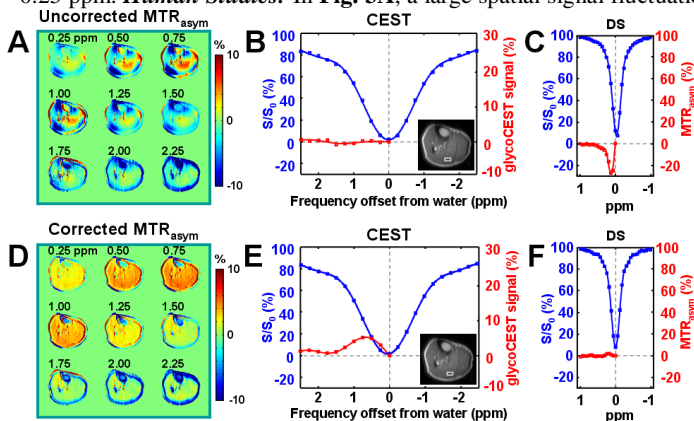


Fig. 3: CEST images, Z-spectra and  $MTR_{asym}$  spectra from human gastrocnemius calf muscle before (A, B, C) and after (D, E, F) correction

frequency reference. WASSR was necessary to obtain proper images of glycogen in both phantoms and *in vivo* human calf muscle and is expected to be beneficial for accurate quantification of CEST effects in tissue. **REFERENCES:** 1) Ward KM, et al. J Magn Reson 2000;143(1):79-87. 2) Zhang S, et al. Acc Chem Res 2003;36(10):783-790. 3) Aime S, et al. Magn Reson Med 2002;47(4):639-648. 4) Yoo B and Pagel MD. J Am Chem Soc 2006;128(43):14032-14033. 5) Zhou J, et al. Nat Med 2003;9(8):1085-1090. 6) van Zijl PC, et al. Proc Natl Acad Sci USA 2007;104(11):4359-4364. 7) Webb P, et al. Mag Reson Med 1992;23(1):1-11. **GRANTS SUPPORT:** NIH-NCRR P41-RR15241, NIH-NIBIB R01-EB02634, R21-EB02666, Philips Medical System.